

# Effect of continuous oscillatory shear on isothermal crystallization of non-nucleated and nucleating-agent-treated isotactic polypropylene assessed by dynamic mechanical analysis

Lan Chen,<sup>1</sup> Chuan-Guo Ma,<sup>2</sup> Hai-Yan Wang,<sup>3</sup> Jin-Xiu Zhang,<sup>1</sup> Xiao-Min Xiong<sup>1,4</sup>

<sup>1</sup>School of Physics and Engineering, Sun Yat-sen University, Guangzhou 510275, China

<sup>2</sup>School of Material Science and Engineering, Guilin University of Electronic Technology, Guilin 541004, China

<sup>3</sup>Guangzhou Institute of Measurement and Testing Technology, Guangzhou, Guangdong 510663, China

<sup>4</sup>State Key Laboratory of Optoelectronic Materials and Technologies, School of Physics & Engineering, Sun Yat-Sen University, Guang Zhou 510275, China

Correspondence to: X.-M. Xiong (E-mail: xiongxm@mail.sysu.edu.cn)

**ABSTRACT:** Using dynamic mechanical analysis (DMA), we investigated the *in situ* crystallization kinetics of non-nucleated and nucleating-agent-treated isotactic polypropylene (*i*PP) under continuous oscillatory shear during the entire crystallization process, and then compared the DMA results with those measured using differential scanning calorimetry under conventional quiescent crystallization. Our analyses, based on the Avrami equation, show that continuous oscillatory shear accelerated crystallization of non-nucleated *i*PP, but interfered with crystallization for nucleating-agent-treated *i*PP. Our results indicate that, for the present nucleating agent, its accelerating effect on crystallization cannot coexist with the accelerating effect of shear on crystallization. We attributed this difference to the disruptive effect of shear on growth and the different nucleation models of non-nucleated and nucleating-agent-treated *i*PP. © 2014 Wiley Periodicals, Inc. *J. Appl. Polym. Sci.* **2015**, *132*, 41685.

**KEYWORDS:** crystallization; kinetics; mechanical properties

Received 30 June 2014; accepted 25 October 2014

DOI: 10.1002/app.41685

## INTRODUCTION

Isotactic polypropylene (*i*PP) is a semi-crystalline polymer that is widely used for its excellent mechanical properties, high malleability, and strong corrosion resistance.<sup>1–4</sup> Generally, *i*PP has three crystalline phases: monoclinic ( $\alpha$ ), hexagonal ( $\beta$ ), and orthorhombic ( $\gamma$ ).  $\alpha$ -phase *i*PP has relatively large modulus but poor extensibility, while  $\beta$ -phase *i*PP has high ductility but low stiffness.<sup>1,5,6</sup> In usual industrial conditions,  $\alpha$ -phase *i*PP is mostly obtained for it is thermodynamically stable. The addition of some content of  $\beta$ -phase *i*PP will largely improve the mechanical properties of products.

$\beta$ -phase *i*PP is thermodynamically metastable and difficult to obtain under normal processing conditions. To promote the formation of  $\beta$ -phase *i*PP, it is common to add a nucleating agent.<sup>6</sup> The nucleating agent might be a nanocomposite with high interfacial area, which can greatly influence the crystalline properties even at rather low filler loading. In our previous work, we used irradiation graft polymerization to modify non-layered calcium carbonate (CaCO<sub>3</sub>) nanoparticles, which we mechanically compounded with polypropylene.<sup>7</sup> Another way to

induce the  $\beta$ -phase is by applying shear during early crystallization.<sup>8–15</sup> Applying shear causes the molecular chains to orient into  $\alpha$  row nuclei, which can induce  $\beta$ -phase crystals. Huo<sup>16</sup> investigated the relationship between the additive content, applied shear, and the formation of  $\beta$ -phase PP, finding that in PP with low additive content (in Huo's case, a mixture of lanthanum stearate and CaCO<sub>3</sub>), shear induced the formation of  $\beta$ -phase crystals in almost the same proportion as in non-nucleated *i*PP. In contrast, for the samples with high additive content, the formation of the  $\beta$ -phase was caused by the nucleating agent. Thus, shear restrained the formation of high amounts of  $\beta$ -phase for the melt with an additive.

However, in most previous work, one-directional or oscillatory shear was applied only during the first seconds of isothermal crystallization while the sample was still molten. Furthermore, the stress generated due to differential thermal contraction of the two components, exerts a kind of force on crystallizing PP melt, which in turn causes variation of nucleation rate and formation of transcrystallization of PP on the surface of already formed nylon6 spherulites on reaching the temperature suitable for crystallization of PP in PP/nylon6 blend, during the

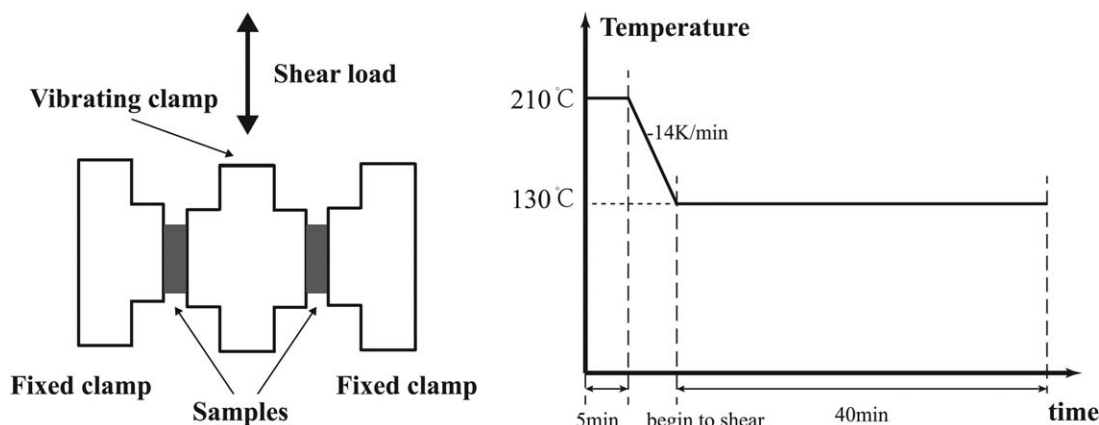


**Figure 1.** (a) Schematic of shear mode in DMA/SDTA861e; (b) Synoptic path of isothermal crystallization at 130°C in the DMA experiments.

nonisothermal crystallization.<sup>17</sup> Dynamic mechanical analysis (DMA) is a new way to investigate the *in situ* crystallization behavior under continuous oscillatory shear for the entire process.<sup>18,19</sup> In our previous work,<sup>19</sup> we reported the influence of oscillatory shear on crystallization of *i*PP in a multifrequency mode. Compared with other techniques, which usually provide one-directional shear during early crystallization, DMA offers vertical periodical shear that is continuous throughout the entire crystallization process.

In the present work, we used DMA to investigate the crystallization kinetics of non-nucleated and nucleating-agent-filled *i*PP under continuous oscillatory shear over the entire crystallization process. We compared these results with those measured using differential scanning calorimetry (DSC) of conventional quiescent crystallization. We wished to clarify the effect of continuous oscillatory shear on crystallization in two different materials. On the basis of the Avrami equation, the crystallization kinetics is analyzed.

## EXPERIMENTAL

### Materials

Commercial *i*PP F1401 (Guangzhou Petrochemical, China) was used with a melt flow index of  $\sim 2.75$  g/10 min (230°C/2.16 kg, ASTM D1238) and an average  $M_n$  and  $M_w$  of  $\sim 6.5 \times 10^4$  and  $\sim 3.3 \times 10^5$  g/mol, respectively. The specimens for the DMA tests comprised a couple round plates ( $\Phi 10 \times 1.0$  mm) prepared by compression molding at 200°C under 7 MPa. Samples treated with a nucleating agent (denoted as *i*PP1) were prepared by introducing 1.96 vol % of stearic-acid-coated CaCO<sub>3</sub> particles (40 nm) during mixing at 200°C for 15 min.<sup>20</sup>

### Characterization

DMA (DMA/SDTA861, Mettler-Toledo GmbH, Switzerland) was performed in shear mode in a nitrogen atmosphere. In these experiments, two identical samples were clamped symmetrically between two outer fixed parts, and the central moving part provided the oscillatory force [Figure 1(a)].

Figure 1(b) shows the synoptic pathway of the DMA measurements. The specimens were heated from room temperature to 210°C at 20°C/min and then held for 5 min to eliminate the thermal history. The specimens were then cooled at 14°C/min

(the fastest cooling rate of the machine) to 130°C and then held for 40 min, allowing isothermal crystallization and DMA measurements to occur simultaneously. The shear load was applied to the polymer melt immediately after the temperature dropped to 130°C. The upper limit of the displacement amplitude was 200  $\mu\text{m}$ , and the upper limit of the shear load was 5 N. The shear rate corresponding to 10 Hz is  $2.67 \text{ s}^{-1}$ .

Quiescent crystallization experiments (DSC 7, Perkin-Elmer, USA) were performed in a nitrogen atmosphere. The temperatures program used in DSC experiments was exactly the same as in the DMA experiments, except that shear force was not applied in DSC.

## RESULTS AND DISCUSSION

### Effect of Nucleating Agent on Quiescent Isothermal Crystallization of *i*PP at 130°C

Figure 2 shows the DSC curves of *i*PP and *i*PP1 undergoing quiescent isothermal crystallization at 130°C. The crystallization peak of non-nucleated *i*PP at  $t_0 = 556$  s differed from that of *i*PP1 at  $t_0 = 130$  s, indicating that the nucleating agent

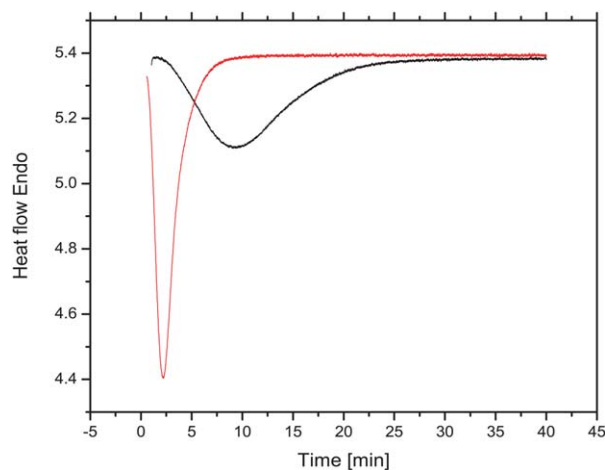


**Figure 2.** DSC curves of quiescent isothermal crystallization of non-nucleated *i*PP (black) and *i*PP1 with  $\beta$ -nucleating agent (red) at 130°C. [Color figure can be viewed in the online issue, which is available at wileyonlinelibrary.com.]

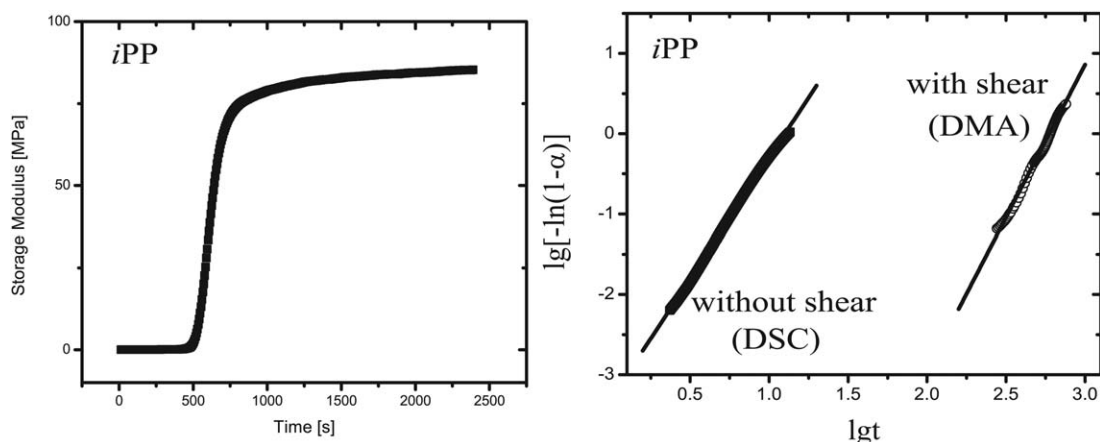


**Figure 3.** (a) Storage modulus of non-nucleated *iPP* during isothermal crystallization under oscillatory shear at 130°C. The measuring frequency was 10 Hz. (b) Avrami relation of isothermal crystallization of non-nucleated *iPP* under quiescent crystallization (■) and oscillatory shear (○) at 130°C.

accelerated crystallization. We found almost no induction period in either curve because the profile of the DSC experiment is the same as that of the DMA experiment in Figure 1(b), meaning the cooling rate (14°C/min, which is the fastest cooling rate of DMA) was not fast enough.

#### Effect of Oscillatory Shear on Isothermal Crystallization of *iPP* at 130°C

Figure 3(a) shows the storage modulus  $G'(t)$  over time for non-nucleated *iPP* isothermally crystallized at 130°C. The storage modulus remained relatively low until the sample remained at 130°C for over 550 s, suggesting that the *iPP* remained molten until 550 s. With increasing time, the modulus increased rapidly and plateaued at ~800 s, indicating that crystallization had mostly completed.

From the DMA tests, we obtained the time dependence of the storage modulus  $G'(t)$ . Then, we calculated the relative crystallinity  $\alpha$  by introducing the model developed by Budiansky<sup>21,22</sup>:

$$\frac{1-\alpha}{1+\varepsilon(G'_a/G'(t)-1)} + \frac{\alpha}{1+\varepsilon(G'_s/G'(t)-1)} = 1 \quad (1)$$

$$\alpha = \frac{G'(t) - G'_a}{G'_s - G'_a} \times \left[ 1 + \varepsilon \left( \frac{G'_s}{G'(t)} - 1 \right) \right]$$

where  $G'_a$  and  $G'_s$  are the shear modulus of the amorphous and spherulitic phases, respectively. The constant  $\varepsilon$  is 0.4 for PP.<sup>22</sup> From these results, we calculated the half-time  $\tau_{1/2}$  with  $\alpha = 0.5$ .

The time dependence of the crystallinity  $\alpha$  during isothermal crystallization can be expressed by the Avrami equation<sup>23,24</sup>:

$$\lg[-\ln(1-\alpha)] = \lg k + n \lg t \quad (2)$$

where  $n$  is the Avrami exponent and  $k$  is a rate constant. For thermal nucleation, the number of nuclei is changing with time. The Avrami exponent  $n = 2$  indicates one-dimensional growth (fibrillar) with a constant bulk nucleation rate,  $n = 3$  indicates two-dimensional nucleation (planar), and  $n = 4$  indicates three-dimensional nucleation (spherical).

Figure 3(b) shows the Avrami analysis of sheared and quiescent crystallization. Table I shows the half-times  $\tau_{1/2}$  and Avrami

parameters from the DMA and DSC experiments, revealing that the half-time  $\tau_{1/2}$  of *iPP* changed from 1509 s for quiescent crystallization to 555 s for shear crystallization. Thus, the oscillatory shear dramatically increased the crystallization rate.

Furthermore, the Avrami analysis shows that the crystallization mechanism of non-nucleated *iPP* differed dramatically between quiescent and shear crystallization. The Avrami exponent  $n$  of non-nucleated *iPP* was 3 in quiescent crystallization (DSC experiments), which means that the nucleation model of non-nucleated *iPP* is athermal and almost perfect spherical. But in shear crystallization (DMA experiments), the Avrami exponent  $n$  of non-nucleated *iPP* changed to 3.8. It is indicated that the oscillatory shear may influence the nucleating model of crystallization. A possible nucleating mechanism of non-nucleated *iPP* in shear is thermal and between planar and spherical.

This behavior may be caused by two effects of shear on the melt. First,<sup>25,26</sup> shear may affect the orientation of molecule chains to form nuclei, which will induce more nuclei. Second,<sup>27</sup> stress—which crystalline aggregates are subjected to when growing in a sheared melt—not only orients chains in the melt but could also disrupt crystalline aggregates. This disruption introduces more nuclei into the melt, accelerating nucleation.

#### Effect of Oscillatory Shear on the Isothermal Crystallization of *iPP1* at 130°C

Figure 4(a) shows the storage modulus during isothermal crystallization of *iPP1* under oscillatory shear at 130°C, also showing the storage modulus of *iPP* for comparison. These results

**Table I.** Parameters of Data Analysis for the Isothermal Crystallization Experiments of PP and *iPP1*

	Without shear by DSC			With shear by DMA		
	$\tau_{1/2}$ (s)	$n$	$\lg k$	$\tau_{1/2}$ (s)	$n$	$\lg k$
<i>iPP</i>	1509	3.00	-3.31	555	3.80	-10.54
<i>iPP1</i>	130	4.07	-1.70	257	2.41	-5.85

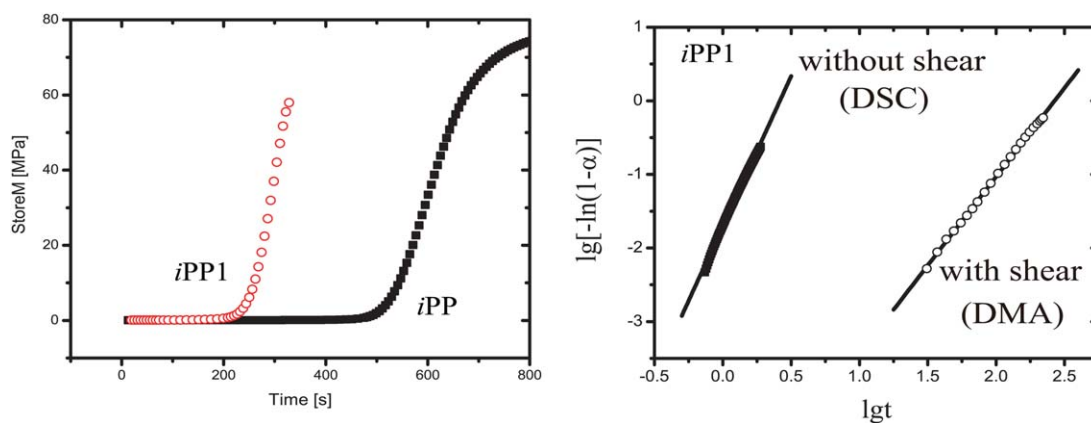


**Figure 4.** (a) Storage modulus of *iPP1* (with nucleating agent) during isothermal crystallization under oscillatory shear at 130°C. The measuring frequency was 10 Hz. For comparison, the storage modulus curve of PP is also given. (b) Avrami relation of isothermal crystallization of *iPP1* under quiescent crystallization (■) and oscillatory shear (○) at 130°C. [Color figure can be viewed in the online issue, which is available at [wileyonlinelibrary.com](http://wileyonlinelibrary.com).]

show that the nucleating agent accelerated crystallization of *iPP1* even with added oscillatory shear.

On the basis of the DSC and DMA results, we calculated the half-time  $\tau_{1/2}$  of *iPP1*, as shown in Table I. The half-time  $\tau_{1/2}$  measured from the DSC experiments was 130 s, much smaller than that measured from the DMA experiment, 257 s. This difference indicates that oscillatory shear interfered with crystallization when a nucleating agent was present, contrasting the results for non-nucleated PP. The Avrami exponent  $n$  decreased from 4.08 (quiescent) to 2.41 (shear), also contrasting the results for non-nucleated PP. It is also indicated that the nucleating model of nucleating-agent-treated *iPP* is thermal and shear causes it changing from spherical ( $n = 4.08$ ) to planar or fibrillar ( $n = 2.41$ ), which is characteristic for sheared melt.

These results may be attributed to shear disrupting the growth process and the different nucleation models of *iPP* and *iPP1*. Crystallization includes both nucleation and growth, but one step may dominate the other. The nucleation model of non-nucleated *iPP* is athermal nucleation, in which the nuclei come from the unmolten chain segments and nucleation dominates. Shear can promote the formation of crystal nucleus in early crystallization, as we discussed in section “Effect of Oscillatory Shear on the Isothermal Crystallization of *iPP1* at 130°C”. Thus, shear accelerates the overall crystallization rate. However, continuous oscillatory shear disrupts growth. The nucleation model of *iPP1* is athermal nucleation too, but in which growth dominates, explaining how shear inhibited the crystallization of *iPP1*.

## CONCLUSIONS

Using DMA and DSC, we investigated the isothermal crystallization behaviors of *iPP* and *iPP1* (*iPP* treated with a nucleation agent) under continuous oscillatory shear and quiescent crystallization. These studies revealed that continuous oscillatory shear accelerated crystallization of *iPP* but interfered with quiescent crystallization of *iPP1*. We analyzed the kinetics of isothermal crystallization by using the Avrami equation. Our results showed that, for *iPP*, continuous oscillatory shear accelerated

the nucleation rate. In contrast, for *iPP1*, it interfered with the growth during crystallization. These results can be explained by assessing the disruptive effect of continuous shear and the different nucleation models of *iPP* and *iPP1*.

## ACKNOWLEDGMENTS

This investigation was supported by National Natural Science Foundation of China (NSFC) (Grant nos. 10974259, 11274391, and 11104357), Science and Technology Planning Project of Guangdong Province, China (Grant no. 2012B060100003), Fundamental Research Funds for the Central Universities (Grant nos. 121gpy36 and 09lgpy29), National Key Technology R&D Program of the Ministry of Science and Technology (2011BAK15B04).

## REFERENCES

- Varge, J. In *Structure and Morphology*; Karger-Kocsis, J., Ed.; Chapman & Hall: London, **1995**, p 56.
- Varge, J.; Ehrenstein, G. W. In *Polypropylene: An A-Z Reference*; Karger-Kocsis, J., Ed.; Kluwer: Dordrecht, **1999**, p 51.
- Iijima, M.; Strobl, G. *Macromolecules* **2000**, *33*, 5204.
- Padden, J.; Keith, H. D. *J. Appl. Phys.* **1959**, *30*, 1479.
- Moore, E. P., Ed. *Polypropylene Handbook: Polymerization, Characterization, Properties, Processing, Applications*; Hanser-Gardner: Cincinnati, **1996**.
- Varga, J. *J. Macromol. Sci. Part B: Phys.* **2002**, *41*, 1121.
- Ma, C. G.; Rong, M. Z.; Zhang, M. Q. *Chin. Chem. Lett.* **2005**, *16*, 409.
- Varga, J.; Karger-Kocsis, J. *J. Polym. Sci. Part B: Polym. Phys.* **1996**, *34*, 657.
- Liu, Q.; Sun, X. L.; Li, H. H.; Yan, S. K. *Polymer* **2013**, *54*, 4404.
- Natalia, V.; Pogodina, H.; Henning, W.; Srivatsan, S. *J. Polym. Sci. Part B: Polym. Phys.* **1999**, *37*, 3512.
- Huo, H.; Jiang, S. C.; An, L. *J. Polymer* **2005**, *46*, 11112.
- Jay, F.; Haudin, J. M.; Monasse, B. *J. Mater. Sci.* **1999**, *34*, 2089.

13. Somani, R. H.; Hsiao, B. S.; Nogales, A.; Srinivas, S.; Tsou, A. H.; Sics, I. *Macromolecules* **2000**, *33*, 9385.
14. Somani, R. H.; Hsiao, B. S.; Nogales, A.; Fruitwala, H.; Srinivas, S.; Tsou, A. H. *Macromolecules* **2001**, *34*, 5902.
15. Nilesh, P.; Carmine, I.; Markus, G.; Sanjay, R. *Polymer* **2013**, *54*, 5883.
16. Huo, H.; Jiang, S.; An, L.; Feng, J. C. *Macromolecules* **2004**, *37*, 2478.
17. Jafari, S. H.; Gupta, A. K. *J. Appl. Polym. Sci.* **1999**, *71*, 1153.
18. Dotsch, T.; Pollard, M.; Wilhelm, M. *J. Phys. Condens. Matter.* **2003**, *15*, S923.
19. Ma, C. G.; Chen, L.; Xiong, X. M.; Zhang, J. X.; Rong, M. Z.; Zhang, M. Q. *Macromolecules* **2004**, *37*, 8829.
20. Ma, C. G.; Mai, Y. L.; Rong, M. Z.; Ruan, W. H.; Zhang, M. Q. *Compos. Sci. Technol.* **2007**, *67*, 2997.
21. Budiansky, B. J. *Mech. Phys. Solids* **1965**, *13*, 223.
22. Alig, I.; Tadjbakhsh, S.; Floudas, G.; Tsisilianis, C. *Macromolecules* **1998**, *31*, 6917.
23. Avrami, M. J. *J. Chem. Phys.* **1939**, *7*, 1103.
24. Wunderlich, B. *Macromolecular Physics*, Vol. 2; Academic Press: New York, **1976**, p 132.
25. Koscher, E.; Fulchiron, R. *Polymer* **2002**, *43*, 6931.
26. Pogodina, N. V.; Lavrenko, V. P.; Srinivas, S.; Winter, H. H. *Polymer* **2001**, *42*, 9031.
27. Masubuchi, Y.; Watanabe, K.; Nagatake, W.; Takimoto, J. I.; Koyama, K. *Polymer* **2001**, *42*, 5023.